

ATMOSPHERIC SCIENCE

Temperature effect on phase state and reactivity controls atmospheric multiphase chemistry and transport of PAHs

Qing Mu,^{1*} Manabu Shiraiwa,^{1,2} Mega Octaviani,^{1*} Nan Ma,^{3,1} Aijun Ding,^{4,5} Hang Su,^{3,1†} Gerhard Lammel,^{1,6†} Ulrich Pöschl,^{1,7} Yafang Cheng^{1,3†}

Polycyclic aromatic hydrocarbons like benzo(*a*)pyrene (BaP) in atmospheric particulate matter pose a threat to human health because of their high carcinogenicity. In the atmosphere, BaP is mainly degraded through a multiphase reaction with ozone, but the fate and atmospheric transport of BaP are poorly characterized. Earlier modeling studies used reaction rate coefficients determined in laboratory experiments at room temperature, which may overestimate/underestimate degradation rates when applied under atmospheric conditions. Moreover, the effects of diffusion on the particle bulk are not well constrained, leading to large discrepancies between model results and observations. We show how regional and global distributions and transport of BaP can be explained by a new kinetic scheme that provides a realistic description of the temperature and humidity dependence of phase state, diffusivity, and reactivity of BaP-containing particles. Low temperature and humidity can substantially increase the lifetime of BaP and enhance its atmospheric dispersion through both the planetary boundary layer and the free troposphere. The new scheme greatly improves the performance of multiscale models, leading to better agreement with observed BaP concentrations in both source regions and remote regions (Arctic), which cannot be achieved by less-elaborate degradation schemes (deviations by multiple orders of magnitude). Our results highlight the importance of considering temperature and humidity effects on both the phase state of aerosol particles and the chemical reactivity of particulate air pollutants.

INTRODUCTION

Polycyclic aromatic hydrocarbons (PAHs) are derived from combustion processes. High health risks are associated with exposure to PAHs, among which benzo(*a*)pyrene (BaP) is one of the most carcinogenic species (1, 2). Because BaP resides almost entirely in the particulate phase, the distribution and long-range atmospheric transport of BaP are largely controlled by its multiphase degradation, mainly the reaction of particulate BaP with gaseous ozone (3). Laboratory studies showed rapid BaP degradation on the surface of soot, ammonium sulfate, and organic aerosol (OA) particles (4–6), whereas atmospheric observations revealed a much longer lifetime and persistence of BaP especially toward remote and polar regions (7, 8). Recent laboratory and kinetic studies have shown that OA coatings can effectively shield BaP from oxidants and that the OA phase state may strongly influence the rate of degradation (9–13). However, key factors controlling the multiphase degradation and the fate of BaP in aerosols under real atmosphere conditions are still not resolved (14). In particular, the laboratory-derived degradation schemes of BaP that have been applied in previous model studies (Fig. 1A and table S1) (14–21) do not fully account for dependence on environmental conditions/parameters.

Temperature (T) and relative humidity (RH) in the atmosphere cover a wide range, which influence not only the phase state and diffusivity of OA (12) but also the chemical reactivity of organic compounds. Because most modeling studies used degradation rates determined at room temperature (that is, 296 to 298 K) in laboratory experiments, they may overestimate degradation rates when applied in colder atmospheric environments. On the basis of the study of Zhou *et al.* (11), Shrivastava *et al.* (14) introduced a threshold temperature below which the OA coating was assumed to shut off the multiphase degradation of BaP. This shielding effect improved agreement between model predictions and observations and was very sensitive to choice of threshold temperature. A simple threshold value, however, does not resolve the actual temperature dependence of multiphase reactions because both the molecular diffusivity and the chemical reactivity of BaP are expected to exhibit a continuous change in response to changing temperature rather than following a step function (13).

Moreover, the effects of diffusion and reaction on the particle bulk are not well characterized in earlier studies. For example, most laboratory experiments (4, 5, 11, 22) were carried out under excessively high ozone concentrations (up to three orders of magnitude above tropospheric levels), and often, surface reaction rate equations were used to extrapolate the laboratory results for application in atmospheric models. The use of surface reaction rate equations without considering bulk processes, however, can result in inconsistent dependencies of BaP degradation rates on RH and ozone concentration (text S1).

Here, we use an advanced kinetic model framework to develop an elaborate kinetic scheme for better representation of multiphase degradation of BaP in regional and global models. This new scheme has incorporated three major improvements compared to previous schemes: (i) considering the formation of reactive oxygen intermediates (ROIs), (ii) including temperature and humidity effects on phase state of OA and temperature-dependent chemical reactivity, and (iii) using a model

¹Multiphase Chemistry Department, Max Planck Institute for Chemistry, P.O. Box 3060, 55128 Mainz, Germany. ²Department of Chemistry, University of California, Irvine, Irvine, CA 92697–2025, USA. ³Institute for Environmental and Climate Research, Jinan University, 511443 Guangzhou, China. ⁴Joint International Research Laboratory of Atmospheric and Earth System Sciences, School of Atmospheric Sciences, Nanjing University, 210023 Nanjing, China. ⁵Jiangsu Provincial Collaborative Innovation Center of Climate Change, 210023 Nanjing, China. ⁶Research Centre for Toxic Compounds in the Environment, Masaryk University, 62500 Brno, Czech Republic. ⁷Johannes Gutenberg University Mainz, 55122 Mainz, Germany. *These authors contributed equally to this work.

†Corresponding author. Email: yafang.cheng@mpic.de (Y.C.); g.lammel@mpic.de (G.L.); h.su@mpic.de (H.S.)

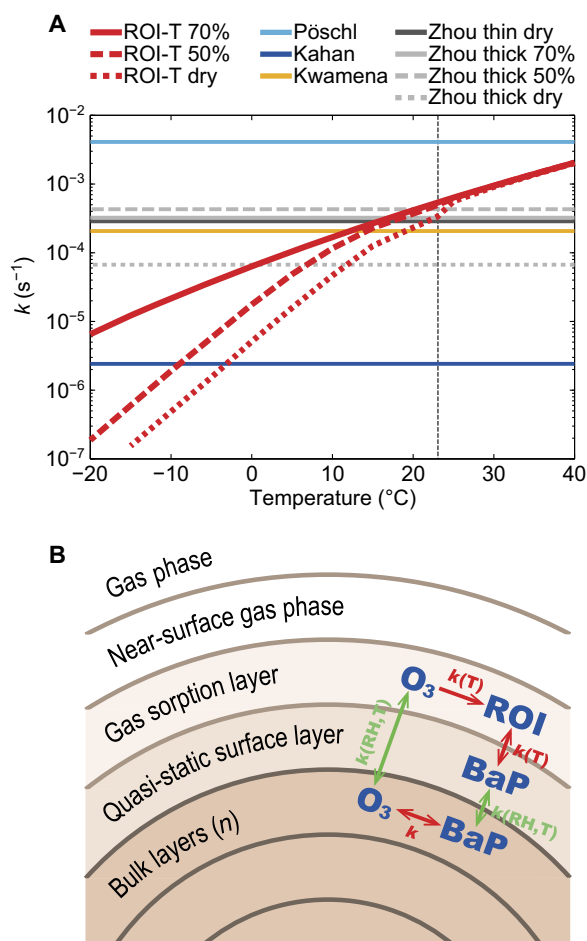


Fig. 1. Kinetic scheme ROI-T. (A) First-order multiphase degradation rate coefficient k (s^{-1}) for laboratory schemes of Pöschl *et al.* (4), Kahan *et al.* (22), Kwamena *et al.* (5), and Zhou *et al.* (11) (table S1) and the kinetic scheme ROI-T at 50 ppb O_3 . Vertical dashed line denotes 23°C. (B) Model framework of the multilayer kinetic scheme ROI-T. Red arrows show the reactions: O_3 is decomposed and forms ROI in the gas sorption layer, BaP reacts with ROI between gas sorption and surface layer, and BaP reacts with O_3 in the bulk. Green arrows show the RH/T-dependent mass transport: O_3 from gas sorption to bulk layer, BaP from bulk to surface layer.

framework that considers both bulk diffusion/reaction and surface reaction to interpret laboratory results for application in models and comparison to field measurements. We find that the new ROI-T scheme can be a good predictor of BaP concentrations from regional to global scales. Our results highlight the importance of temperature in BaP multiphase degradation from a kinetic view and demonstrate a universal scheme that can be applied for various atmospheric conditions and geolocations. Because of the common existence of OA coating, similar temperature effects are expected for other multiphase reactions, which can be determined from laboratory studies by the general modeling framework and approaches proposed here.

RESULTS

BaP degradation kinetic scheme

In the new kinetic scheme ROI-T, the multiphase degradation of BaP with ozone is treated in multiple compartments as shown in Fig. 1B,

which has not yet been fully considered by previous schemes. The reaction involves the decomposition of surface ozone and formation of ROI (23). To account for mass transport and reactions of gaseous and particle-bound chemical species at the surface and in the bulk phase, we apply the kinetic multilayer model of aerosol surface and bulk chemistry (KM-SUB) (24) (see KM-SUB model in Materials and Methods), which is based on the Pöschl-Rudich-Ammann framework (25). Secondary OA (SOA) formed from α -pinene oxidation was chosen to represent the OA coating (11). With the kinetic parameters in table S2, the new kinetic scheme ROI-T can effectively explain the kinetics of multiphase degradation of BaP and successfully reproduce the results of the Zhou's experimental data (11) for both thin and thick coating cases (8 and 40 nm) at different RH (that is, dry, 50% and 70%). In further regional/global model applications, the thick coating scenario is adopted, because the global simulation has found that the OA shielding on BaP is generally thick (14). As shown in Fig. 1A, rather than a fixed degradation rate, the rate coefficients of the ROI-T scheme show a monotonic increase with increasing temperature and systematically smaller degradation rate of BaP at lower RH.

The temperature and RH dependence of diffusivity and BaP chemical reactivity both control the degradation rate of BaP. In the new ROI-T scheme, on the one hand, temperature influences OA diffusivity and its phase state, that is, the diffusion coefficients of ozone and BaP are assumed to decrease by one order of magnitude upon a temperature decrease of 10°C (26) (see KM-SUB model in Materials and Methods). On the other hand, temperature influences the chemical reactivity of BaP with ROI following the Arrhenius equation (see KM-SUB model in Materials and Methods). Considering both effects, the degradation rates of BaP at 253 K are three to four orders of magnitude smaller than those at 313 K (Fig. 1A).

To demonstrate the advantages of the new ROI-T scheme, we have also included other commonly used degradation schemes of BaP: Kwamena *et al.* (5), Kahan *et al.* (22), and Pöschl *et al.* (4) schemes refer to ozonolysis of uncoated BaP on azelaic acid, liquid substrates, and soot, respectively; the Zhou *et al.* (11) scheme refers to ozonolysis of OA-coated BaP. As shown in Fig. 1A, these schemes show different degradation rates due to the substrate and shielding effects summarized in table S1.

Model versus observation

Other BaP degradation schemes provide reliable predictions only at specific characteristic distances from sources or geolocations but are less at others. For example, the Kwamena scheme shows the best agreement with observations at mid-latitude, whereas the optimum scheme for the Arctic is the scheme that predicts the slowest degradation rates, that is, the Kahan scheme (Fig. 1A) (17, 19). The ROI-T scheme, on the contrary, can account for the different temperature/RH regimes at different locations and transport distances.

In Fig. 2A, we compare the performance of the kinetic ROI-T scheme and the most commonly used Kwamena scheme (15, 18, 21, 27) in multiscale model simulations (see Model setup and BaP extension in Materials and Methods). The model results from the Pöschl scheme (the fastest) and the Kahan scheme (the slowest) (Fig. 1A) are also included as references. The observational data used for model evaluation cover a wide range of source/receptor sites over a large span of latitudes (33° to 83°N; see Observational data of BaP in Materials and Methods). Compared with other schemes, the ROI-T scheme consistently provides better predictions at all types of sites, from near-source, mid-latitude, remote background sites to the Arctic (table S4). It improves

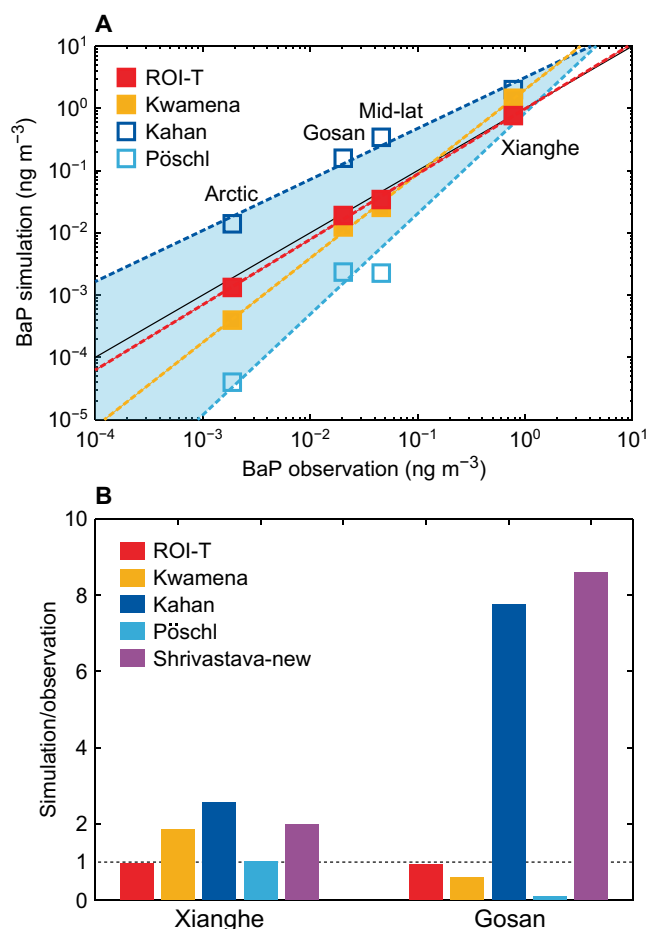


Fig. 2. Comparisons of the ROI-T scheme and previous laboratory-derived schemes with observations. (A) Simulated concentrations of BaP (ng m^{-3}) by the ROI-T, Kwamena, Kahan, and Pöschl schemes at the Xianghe site, the Gosan site, other mid-latitude sites, and the Arctic sites. The solid black line is a 1:1 line of simulation and observation. The dashed lines are fitted by respective simulations. The shaded area is constrained by the Pöschl and Kahan schemes. (B) The ratios of simulated and observed BaP concentrations with different schemes at the Xianghe site and the Gosan site.

the BaP simulation most significantly at the Arctic sites, where air masses underwent the longest and coldest transport processes. For example, simulated BaP levels at the Alert and Spitsbergen sites are improved by more than one order of magnitude with the ROI-T scheme compared with the Kwamena scheme (table S4A).

To further elucidate the advantages of the ROI-T scheme, we focus on two cases with contrasting temperature/RH conditions (Fig. 2B): a near-source site Xianghe (39.80°N , 116.96°E , 45 km southeast of Beijing, China), representing the local surface transport in hot/humid environment in July, and a remote background site Gosan (33.28°N , 126.17°E on the Jeju Island, about 100 km south of the Korean peninsula), representing long-range transport in cold/dry air in February. The results show that it is impossible to reproduce observations for both cases by a fixed degradation rate. The Kwamena scheme is either too slow for the Xianghe summer case or too fast for the Gosan winter case, suggesting strong temperature and humidity effects on the diffusivity and reactivity. The model performance cannot be improved by simply changing for another degradation rate, because a higher (lower) degradation rate will reduce (increase) the BaP concentrations at both

sites. As shown in Fig. 2 (A and B), a scheme with faster degradation rates, such as Pöschl scheme, reduces the BaP concentration to the same level as observations for the Xianghe case but shows a larger underestimation for the Gosan case. We also test the step function setting of the Zhou scheme as in Shrivastava *et al.* (14). It cannot reproduce BaP observations over both cases either, with a very similar performance as the Kahan scheme (the slowest) (Fig. 2B).

By unifying the impact of temperature and RH on diffusivity and reactivity under an elaborate kinetic framework (Fig. 1B), the ROI-T scheme solves the problem with changing BaP degradation rates in response to the changes of environmental conditions (Fig. 1A). Under the new scheme, the hot/humid conditions increase the diffusivity/reactivity and the BaP degradation rate, whereas it is the other way around in the cold/dry environment. Compared with the Kwamena scheme, our ROI-T scheme leads to reduced BaP concentrations at the Xianghe site and elevated BaP concentration at the Gosan site, finally showing good agreements for both cases. The changes in both diffusivity and chemical reactivity contribute to the changes of degradation rate in the new ROI-T scheme. To decouple their effects, we perform sensitivity studies by turning on/off the temperature/RH dependence of diffusivity. At the Gosan site, a fixed degradation rate in ROI-T scheme at room temperature 296 K leads to an underestimation of BaP concentration by a factor of 3. Further tests show that the temperature/RH-induced change of diffusivity would account for ~50% of the improvement in the predicted BaP concentrations, whereas the change of reactivity further contributes to the rest of the ~50% (as shown by the comparison between the “ROI-T at 296 K” and “ROI-T with fixed diffusivity” cases in fig. S1).

East Asia outflow

As one of the largest source regions, the outflow of BaP from East Asia to the downwind regions and remote Pacific Ocean is of international concern (28, 29). Figure 3 (A and B) shows a typical outflow transport of BaP from East Asia in winter (24 February 2003). With the Kwamena scheme, most BaP is bounded in the boundary layer due to fast degradation with an average lifetime of ~2 to 3 hours throughout the whole domain (fig. S2), resulting in very low concentrations above 1 km (Fig. 3A). However, the decrease of degradation rate, which results from the change in temperature and RH during air mass rising (see temperature and RH distribution in fig. S3), is not accounted for. Even when BaP is able to escape out of the boundary layer by large-scale advections associated with cyclones or by convections in mid-latitudes (that is, 35° to 45°N), fast degradation limits dispersion and transport of BaP to the vicinity of the source region. Thus, the transport of BaP with the Kwamena scheme is constrained within the boundary layer, and the long-range transport impacts are limited.

The ROI-T scheme shows a different spatial distribution and transport pathway of BaP, with more BaP distributed at higher altitude. This is because low temperature reduces OA diffusivity and reaction rate of BaP with ROI [“freezing effect”; see three-dimensional (3D) degradation rate k in fig. S2] and thus leads to a much longer lifetime of BaP above 1 km (~2 to 3 hours to more than 20 days; fig. S2), making transport in the free troposphere an efficient pathway. Compared with the Kwamena scheme, 15 times more BaP is lifted by frontal activities and convection to middle troposphere, where strong westerlies/jets cause a fast transport of the plumes to downwind areas (figs. S5 and S6 and text S2) and toward polar region, resulting in much stronger global impacts. At the cross section of 126°E (Fig. 3, A and B), the BaP outflow toward the ocean shows a maximum zonal net flux of $\sim 35 \text{ ng m}^{-2} \text{ s}^{-1}$ in

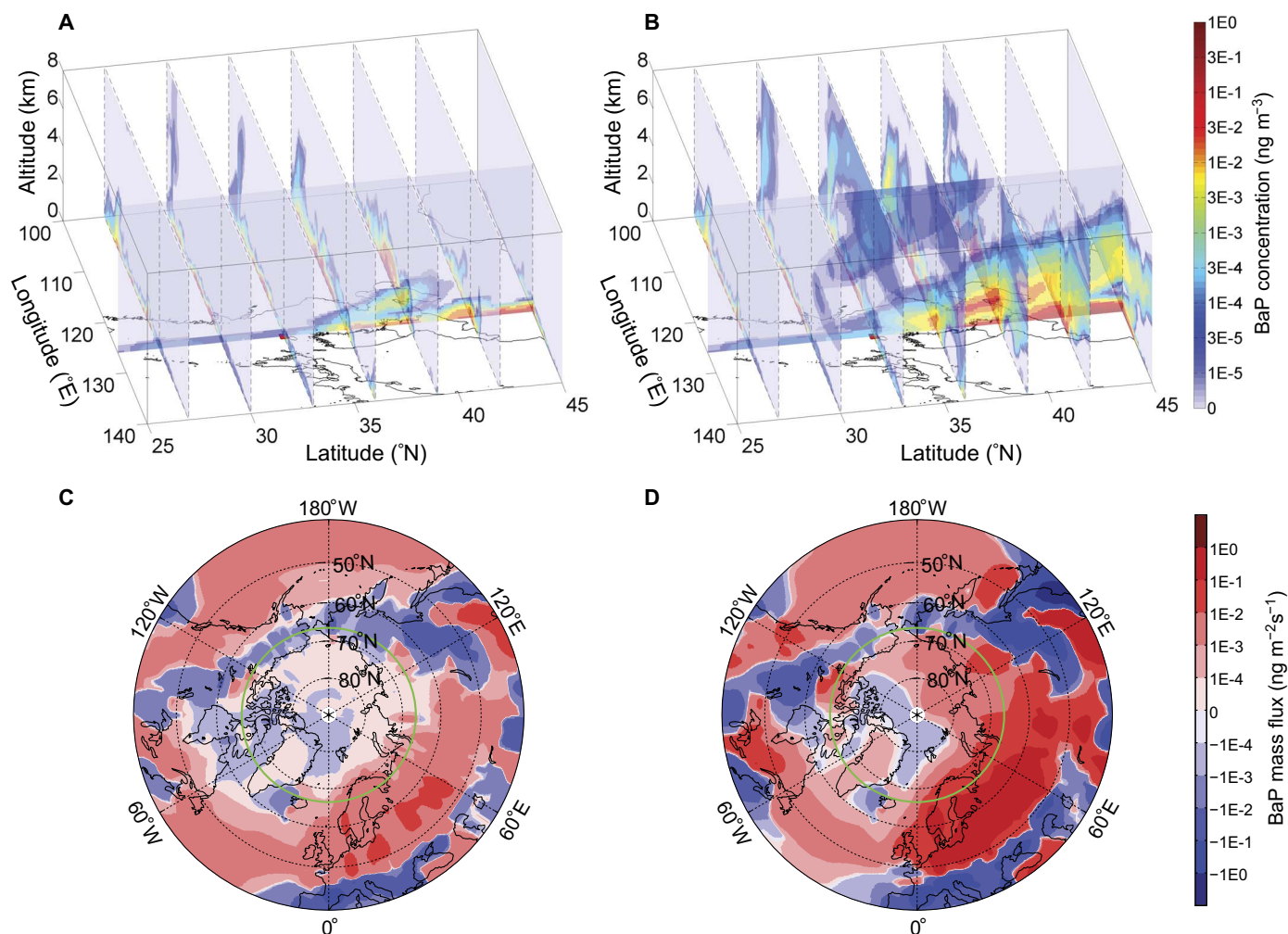


Fig. 3. Implications on the transport. Average concentrations of BaP (ng m^{-3}) in a strong East Asia outflow episode on 24 February 2003 are shown for the (A) Kwamena scheme and the (B) ROI-T scheme. Longitude cross section locates at 126°E . BaP net meridional flux ($\text{ng m}^{-2} \text{s}^{-1}$) averaged over years 2007–2009 are shown for the (C) Kwamena scheme and the (D) ROI-T scheme. Northward has positive values (red), and southward has negative values (blue). Green circle marks the Arctic Circle at 66.56°N .

the ROI-T scheme but only $\sim 10 \text{ ng m}^{-2} \text{ s}^{-1}$ in the Kwamena scheme (fig. S4, A and B). It is also clear that the vertical center of the BaP column mass in the ROI-T scheme is higher than that in the Kwamena scheme, that is, ~ 0.6 and 0.3 km , respectively (fig. S4, C and D).

Transport to the Arctic

BaP emitted in source regions can undergo intercontinental transport, allowing them to distribute and accumulate even in the polar regions (7, 30). The concentration level of BaP in the Arctic arouses high interest, because BaP is not only a good indicator of human contamination (30) but also responsible for the severe bioconcentrate effect in the Arctic (31) where the ecosystem is most vulnerable, bioaccumulation along marine and terrestrial food chains (31–33). As shown in the East Asia outflow case, the “freezing effect” may make the intercontinental transport of BaP from source regions to the Arctic at high-altitude or low-temperature regions more efficient than previously thought.

As shown in Fig. 3 (C and D), BaP in the Arctic is mainly transported from Europe, North America, and Asia, similar to long-lived halogenated pollutants (34). The 2007–2009 average total meridional net flux of BaP toward the Arctic (integrated over 1000 to

10 hPa at 65°N) is $1.97 \text{ ng m}^{-2} \text{ s}^{-1}$ with the ROI-T scheme but only $0.12 \text{ ng m}^{-2} \text{ s}^{-1}$ with the Kwamena scheme (fig. S4E), which is about 16 times lower. The larger fluxes of BaP with the ROI-T scheme can be attributed to a longer lifetime of BaP caused by the “freezing effect” (fig. S2), because the pollutant is transported significantly higher. The average vertical center of the BaP column mass transported across 65°N during 2007–2009 is 2 km for the ROI-T scheme but only 0.5 km for the Kwamena scheme (fig. S4F), showing a more prominent difference in height than that in the East Asian outflow case.

DISCUSSION

The strong temperature/RH effects on fate and global transport of BaP advance the understanding and challenge the traditional view of modeling the multiphase degradation of reactive pollutants (for example, BaP) in OAs. In warm/humid environments (for example, tropical rainforests), aerosol particles tend to be liquid, whereas in cold environments, aerosols are found to be in an amorphous solid phase, most probably a glassy state (12). The phase state and degradation rate of BaP may vary largely depending on temperature/RH

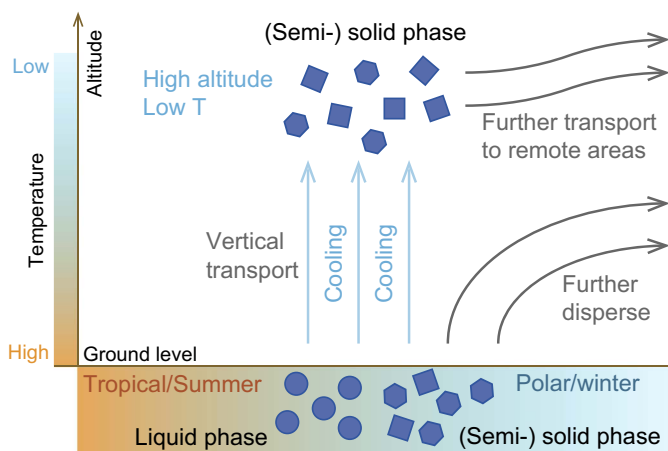


Fig. 4. Diagram of temperature/RH effects on BaP transport in ambient air. OA diffusivity and chemical reactivity are both reduced in response to changes in season (summer to winter), latitude (tropical to polar), and altitude (surface to high altitude), when OA phase state also changes from liquid to (semi-) solid phase. With a slower degradation rate and hence prolonged lifetime, BaP can be further dispersed and transported.

and hence the season (summer versus winter), altitude (surface versus high altitude), and latitude (tropical versus polar) (Fig. 4). It also emphasizes the importance of higher altitude or cold season/region pathway for the long-range transport, that is, the low temperature helps OA and reactive compounds within it survive from the multiphase chemistry, remaining undergraded and being transported further.

The ROI-T scheme is based on the kinetic data observed on the ozonolysis of BaP coated by α -pinene SOA. Recent studies have suggested that α -pinene SOA is less viscous than aromatic SOA and is more viscous than isoprene SOA (35, 36). SOA particles are also often internally mixed with inorganic components, which may affect particle phase state, nonideal mixing and morphology, and hence the multiphase reaction rates (37). Therefore, the effects of different SOA precursors and inorganic interactions should be further explored. Partitioning of PAHs to other OAs, such as bioparticles, is less efficient than partitioning to liquid and semisolid SOA (38). The presence of more viscous bioparticles will lead to less reactive PAHs and therefore an even higher long-range transport potential.

The large impact of temperature/RH on the diffusivity/reactivity is not limited to the degradation of BaP but has general implications for all kinds of multiphase reactions in aerosols, clouds, and fog droplets relevant for atmospheric chemistry and transport (9, 12, 39, 40). The impact is particularly important for the northern hemisphere, where efficient large-scale advection/convection associated with cyclones and strongest anthropogenic emissions exist. Our results demonstrate that it is important to perform laboratory kinetic studies on the large temperature/RH span relevant for atmospheric conditions. Our modeling scheme provides an advanced physicochemical-based framework for the representation of multiphase reaction in atmospheric models and can be readily modified to include other hazardous air pollutants and OA species once the kinetic data are available.

MATERIALS AND METHODS

Model setup

The ROI-T scheme was incorporated as a look-up table (table S3) into two state-of-the-art models with BaP extension for further application.

Regional model

The open-source community model WRF-Chem (Weather Research and Forecasting model coupled with Chemistry), an “online” regional model with coupled meteorology and chemistry (41, 42), has higher spatial resolution and greater advantages in determining the fine structures of transport process, especially the vertical transport within and out of the boundary layer. The PAH extension was based on the model version 3.6.1.

The physics schemes of the regional WRF-Chem model used here were as follows (42): microphysics and cumulus parameterizations followed the Purdue-Lin scheme and the Grell 3D ensemble scheme, respectively. The longwave and shortwave radiations were calculated by the online rapid radiative transfer model and the Goddard scheme, respectively. The planetary boundary layer was based on the Mellor-Yamada-Janjic scheme, along with the Eta similarity surface layer scheme. The implemented air-soil gas exchange was coupled with the Noah land surface model. Photolysis rates used the Fast-J photolysis scheme. As for the chemistry schemes, we used the Regional Atmospheric Chemistry Mechanism (RACM) for homogeneous gas-phase reactions. The aerosol module included the inorganic fraction Modal Aerosol Dynamics model for Europe (MADE) and organic fraction Secondary Organic Aerosol Model (SORGAM).

Global model

The global model EMAC (ECHAM/MESy Atmospheric Chemistry) covered intercontinental transport, such as from source areas to the Arctic. It was a combination of the ECHAM5 general circulation model (43) and MESy (Modular Earth Submodel System, version 2.5) (44). MESy provided infrastructure to couple the base model ECHAM5 and different components (or submodels) that represent various processes of the Earth system.

The model simulations included the following MESy submodels (44): CLOUD described cloud scheme and precipitation. Convection parameterization and radiation were in submodels CONVECT and RAD. Air-sea exchange was parameterized by AIRSEA. Wet and dry depositions were described by SCAV and DDEP. Prescribed emissions were calculated by OFFLEM, whereas online emissions were calculated by ONLEM. As for chemistry, MECCA was responsible for gas-phase chemistry, JVAL took care of photolysis rate, and GMXe was the submodel for aerosol microphysics and semivolatile inorganic partitioning.

Simulation

We performed regional (global) simulations at a grid spacing of 27 km \times 27 km ($1.9^\circ \times 2.5^\circ$) with 39 (19) vertical levels from the surface to 100 hPa (10 hPa). Simulations were conducted during 11 to 22 July 2013 for Xianghe case and 14 to 25 February 2003 for Gosan case over East Asia domain (15° to 55° N, 95° to 155° E) by the regional model, and 2007 to 2009 for mid-latitude and Arctic sites by the global model, respectively.

BaP extension

The following processes of BaP were included: emission, gas-particle partitioning, gas-phase and multiphase reactions, air-soil gas exchange, and wet and dry depositions.

Emissions

Anthropogenic BaP emissions were regridded from a $0.1^\circ \times 0.1^\circ$ global annual PAH emission inventory, with 69 detailed source types (45). Monthly variation was based on black carbon (BC) emission seasonality of HTAP_v2.2 (46). For regional simulations, annual scaling factors (45) and diurnal cycle (following BC) of the PAH emissions were also applied. Biogenic contributions to PAH emission have been neglected.

Gas-particle partitioning

Gas-particle partitioning of BaP used in the regional model followed an equilibrium partitioning expression that accounted for the absorption into organic matter and adsorption onto BC (47, 48). In the global model, polyparameter linear free energy relationships were applied, which accounted for BaP absorption into organic matter and adsorption to soot and inorganic salts (38).

Gas-phase reaction

The second-order rate coefficients for reactions of gaseous BaP with OH, NO₃, and O₃ are 1.5×10^{-10} , 5.4×10^{-11} , and 2.6×10^{-17} cm³ molecules⁻¹ s⁻¹, respectively (49).

Wet/dry depositions

The original regional/global model routines have been adapted to include the deposition of gas-phase and particulate-phase BaP using corresponding deposition parameterizations.

Air-soil gas exchange

Air-soil gas exchange of BaP was parameterized (50) on the basis of air/soil concentrations and properties of BaP. The concentrations of BaP in soil were initialized by the global multicompartmental model ECHAM5-HAM: BaP has been globally simulated over 10 years with 2.8° × 2.8° horizontal resolution (51). A steady state of BaP concentrations in the soil compartment was safely reached.

KM-SUB model

The KM-SUB model treats mass transport and chemical reactions at the surface and in the particle bulk (24). KM-SUB was composed of the following compartments: gas phase, near-surface gas phase, sorption layer, quasi-static surface layer, near-surface bulk layer, and a number of bulk layers. The model resolved the following processes explicitly: gas-phase diffusion, reversible adsorption of O₃, surface reaction involving decomposition of O₃ and formation of long-lived ROIs, bulk diffusion of O₃ and BaP in OA coating, and bulk reaction between O₃ and BaP. Note that heat transfer was not treated in the model because heat released by trace gas uptake and reactions can be efficiently buffered by the ambient gas and did not lead to a substantial increase of particle-surface temperature (52). KM-SUB can simulate the evolution of species at the particle surface and in the particle bulk, along with surface concentrations and gas uptake coefficients. Core-shell morphology was assumed with an organic phase embedding BaP as particle shell and an inorganic phase as particle core (37). The required kinetic parameters were summarized in table S2, and the values were on the basis of previous studies of KM-SUB applications to experimental data of Zhou *et al.* (11).

The ROI-T considered the temperature dependence of bulk diffusivity and chemical reactivity. The diffusion coefficients of ozone and PAH were assumed to decrease by one order of magnitude upon a decrease of temperature by 10°C based on the Vogel-Fulcher-Tamman approach (26, 35). Temperature dependence of rate coefficients *k* was considered by the Arrhenius equation using the activation energies of surface reactions as listed in table S2. KM-SUB simulations were conducted in the temperature range of -20° to 40°C with gas-phase ozone concentrations of 0 to 200 parts per billion (ppb). The obtained first-order decay rate of PAH was then fitted with the Hill equation as shown in table S3, so that the parameterizations can be efficiently incorporated in regional and global transport models.

Observational data of BaP

The near-source observation data of BaP were collected at the Xianghe Atmospheric Observatory (39.80°N, 116.96°E). The Xianghe site is a

suburban site, located 45 km southeast of Beijing and 70 km northwest of Tianjin. Particulate- and gas-phase samples were collected for daytime (8:00 to 18:00 local time) and nighttime (20:00 to 6:00 local time), respectively, during 11 to 22 July 2013.

The outflow observation data of BaP were measured at the Gosan site (33.28°N, 126.17°E) on Jeju Island. The site was 72 m above sea level and about 100 km south of the Korean peninsula. Gosan is a representative background station in East Asia to study outflow of air pollutants from land to ocean. Intensive daily measurements (8:00 to 8:00 local time in the following morning) of particulate phase BaP were carried out during a pollution period 14 to 25 February 2003. Details of sampling and analysis methods were given in the study of Kim *et al.* (53).

The mid-latitude observation data of BaP were taken from 18 stations of the European Monitoring and Evaluation Programme (EMEP) (54), the Integrated Atmospheric Deposition Network (55), and Arctic Monitoring and Assessment Programme (AMAP) (56). Three Arctic sites (that is, north of 66.5°N) are as follows: Alert in Canada (AMAP; 62.3°W, 82.5°N), Spitsbergen in Norway (EMEP; 11.9°E, 78.9°N), and Pallas in Finland (EMEP; 24.3°E, 68.0°N). The concentration of BaP during 2007–2009 was averaged over all months, with at least 1 weekly measurement reported.

SUPPLEMENTARY MATERIALS

Supplementary material for this article is available at <http://advances.sciencemag.org/cgi/content/full/4/3/eaap7314/DC1>

text S1. Problems without considering bulk processes.

text S2. Warm conveyor belts (WCBs) and BaP transport in Gosan winter case.

table S1. Flow tube experiments of multiphase degradation of BaP with ozone.

table S2. Kinetic parameters used in the KM-SUB simulation for the ozonolysis of BaP to reproduce experiment results of the Zhou scheme.

table S3. Parameterization of multiphase degradation rate for the ozonolysis of BaP.

table S4. Comparisons of observed and predicted BaP concentrations in the regional WRF-Chem model and the global EMAC model.

fig. S1. Same as Fig. 2B but with three more sensitivity studies.

fig. S2. Multiphase degradation rate and chemical lifetime.

fig. S3. BaP concentrations and multiphase degradation rate.

fig. S4. Net meridional mass flux and vertical center of column mass for BaP in different cases.

fig. S5. BaP transport due to WCB and frontal activities associated with mid-latitude cyclones for the Gosan winter case.

fig. S6. A conceptual scheme for air pollution transport due to middle-latitude cyclone.

References (57–60)

REFERENCES AND NOTES

1. F. P. Perera, Environment and cancer: Who are susceptible? *Science* **278**, 1068–1073 (1997).
2. P. Boffetta, N. Jourenkova, P. Gustavsson, Cancer risk from occupational and environmental exposure to polycyclic aromatic hydrocarbons. *Cancer Causes Control* **8**, 444–472 (1997).
3. I. J. Keyte, R. M. Harrison, G. Lammel, Chemical reactivity and long-range transport potential of polycyclic aromatic hydrocarbons—A review. *Chem. Soc. Rev.* **42**, 9333–9391 (2013).
4. U. Pöschl, T. Letzel, C. Schauer, R. Niessner, Interaction of ozone and water vapor with spark discharge soot aerosol particles coated with benzo[*a*]pyrene: O₃ and H₂O adsorption, benzo[*a*]pyrene degradation, and atmospheric implications. *J. Phys. Chem. A* **105**, 4029–4041 (2001).
5. N.-O. A. Kwamena, J. A. Thornton, J. P. D. Abbatt, Kinetics of surface-bound benzo[*a*]pyrene and ozone on solid organic and salt aerosols. *J. Phys. Chem. A* **108**, 11626–11634 (2004).
6. S. Zhou, A. K. Y. Lee, R. D. McWhinney, J. P. D. Abbatt, Burial effects of organic coatings on the heterogeneous reactivity of particle-borne benzo[*a*]pyrene (BaP) toward ozone. *J. Phys. Chem. A* **116**, 7050–7056 (2012).
7. C. J. Halsall, L. A. Barrie, P. Fellin, D. C. G. Muir, B. N. Billeck, L. Lockhart, F. Ya. Rovinsky, E. Ya. Kononov, B. Pastukhov, Spatial and temporal variation of polycyclic aromatic hydrocarbons in the Arctic atmosphere. *Environ. Sci. Technol.* **31**, 3593–3599 (1997).

8. C. Schauer, R. Niessner, U. Pöschl, Polycyclic aromatic hydrocarbons in urban air particulate matter: Decadal and seasonal trends, chemical degradation, and sampling artifacts. *Environ. Sci. Technol.* **37**, 2861–2868 (2003).
9. M. Shiraiwa, M. Ammann, T. Koop, U. Pöschl, Gas uptake and chemical aging of semisolid organic aerosol particles. *Proc. Natl. Acad. Sci. U.S.A.* **108**, 11003–11008 (2011).
10. T. Berkemeier, S. S. Steimer, U. K. Krieger, T. Peter, U. Pöschl, M. Ammann, M. Shiraiwa, Ozone uptake on glassy, semi-solid and liquid organic matter and the role of reactive oxygen intermediates in atmospheric aerosol chemistry. *Phys. Chem. Chem. Phys.* **18**, 12662–12674 (2016).
11. S. Zhou, M. Shiraiwa, R. D. McWhinney, U. Pöschl, J. P. D. Abbatt, Kinetic limitations in gas-particle reactions arising from slow diffusion in secondary organic aerosol. *Faraday Discuss.* **165**, 391–406 (2013).
12. M. Shiraiwa, Y. Li, A. P. Tsimplidi, V. A. Karydis, T. Berkemeier, S. N. Pandis, J. Lelieveld, T. Koop, U. Pöschl, Global distribution of particle phase state in atmospheric secondary organic aerosols. *Nat. Commun.* **8**, 15002 (2017).
13. T. Koop, J. Bookhold, M. Shiraiwa, U. Pöschl, Glass transition and phase state of organic compounds: Dependency on molecular properties and implications for secondary organic aerosols in the atmosphere. *Phys. Chem. Chem. Phys.* **13**, 19238–19255 (2011).
14. M. Shrivastava, S. Lou, A. Zelenyuk, R. C. Easter, R. A. Corley, B. D. Thrall, P. J. Rasch, J. D. Fast, S. L. Massey Simonich, H. Shen, S. Tao, Global long-range transport and lung cancer risk from polycyclic aromatic hydrocarbons shielded by coatings of organic aerosol. *Proc. Natl. Acad. Sci. U.S.A.* **114**, 1246–1251 (2017).
15. V. Matthias, A. Aulinger, M. Quante, CMAQ simulations of the benzo(a)pyrene distribution over Europe for 2000 and 2001. *Atmos. Environ.* **43**, 4078–4086 (2009).
16. A. Aulinger, V. Matthias, M. Quante, An approach to temporally disaggregate benzo(a)pyrene emissions and their application to a 3D Eulerian atmospheric chemistry transport model. *Water Air Soil Pollut.* **216**, 643–655 (2011).
17. C. L. Friedman, N. E. Selin, Long-range atmospheric transport of polycyclic aromatic hydrocarbons: A global 3-D model analysis including evaluation of Arctic sources. *Environ. Sci. Technol.* **46**, 9501–9510 (2012).
18. R. San José, J. L. Pérez, M. S. Callén, J. M. Lopez, A. Mastral, BaP (PAH) air quality modelling exercise over Zaragoza (Spain) using an adapted version of WRF-CMAQ model. *Environ. Pollut.* **183**, 151–158 (2013).
19. C. L. Friedman, J. R. Pierce, N. E. Selin, Assessing the influence of secondary organic versus primary carbonaceous aerosols on long-range atmospheric polycyclic aromatic hydrocarbon transport. *Environ. Sci. Technol.* **48**, 3293–3302 (2014).
20. C. L. Friedman, Y. Zhang, N. E. Selin, Climate change and emissions impacts on atmospheric PAH transport to the Arctic. *Environ. Sci. Technol.* **48**, 429–437 (2014).
21. C. I. Efstathiou, J. Matejčičová, J. Bieser, G. Lammel, Evaluation of gas-particle partitioning in a regional air quality model for organic pollutants. *Atmos. Chem. Phys.* **16**, 15327–15345 (2016).
22. T. F. Kahan, N.-O. A. Kwamena, D. J. Donaldson, Heterogeneous ozonation kinetics of polycyclic aromatic hydrocarbons on organic films. *Atmos. Environ.* **40**, 3448–3459 (2006).
23. M. Shiraiwa, Y. Sosedova, A. Rouvière, H. Yang, Y. Zhang, J. P. D. Abbatt, M. Ammann, U. Pöschl, The role of long-lived reactive oxygen intermediates in the reaction of ozone with aerosol particles. *Nat. Chem.* **3**, 291–295 (2011).
24. M. Shiraiwa, C. Pfrang, U. Pöschl, Kinetic multi-layer model of aerosol surface and bulk chemistry (KM-SUB): The influence of interfacial transport and bulk diffusion on the oxidation of oleic acid by ozone. *Atmos. Chem. Phys.* **10**, 3673–3691 (2010).
25. U. Pöschl, Y. Rudich, M. Ammann, Kinetic model framework for aerosol and cloud surface chemistry and gas-particle interactions? Part 1: General equations, parameters, and terminology. *Atmos. Chem. Phys.* **7**, 5989–6023 (2007).
26. A. M. Arangio, J. H. Slade, T. Berkemeier, U. Pöschl, D. A. Knopf, M. Shiraiwa, Multiphase chemical kinetics of OH radical uptake by molecular organic markers of biomass burning aerosols: Humidity and temperature dependence, surface reaction, and bulk diffusion. *J. Phys. Chem. A* **119**, 4533–4544 (2015).
27. A. Aulinger, V. Matthias, M. Quante, Introducing a partitioning mechanism for PAHs into the Community Multiscale Air Quality modeling system and its application to simulating the transport of benzo(a)pyrene over Europe. *J. Appl. Meteorol. Climatol.* **46**, 1718–1730 (2007).
28. Y. Zhang, S. Tao, J. Ma, S. Simonich, Transpacific transport of benzo(a)pyrene emitted from Asia. *Atmos. Chem. Phys.* **11**, 11993–12006 (2011).
29. Y. Zhang, H. Shen, S. Tao, J. Ma, Modeling the atmospheric transport and outflow of polycyclic aromatic hydrocarbons emitted from China. *Atmos. Environ.* **45**, 2820–2827 (2011).
30. V. Hoyau, J. L. Jaffrezo, Ph. Garrigues, M. P. Clain, P. Masclat, Deposition of aerosols in polar regions-contamination of the ice sheet by polycyclic aromatic hydrocarbons. *Polycycl. Aromat. Compd.* **8**, 35–44 (1996).
31. R. W. Macdonald, J. M. Bowers, Contaminants in the arctic marine environment: Priorities for protection. *Ices J. Mar. Sci.* **53**, 537–563 (1996).
32. R. K. Achazi, C. A. M. Van Gestel, Uptake and Accumulation of PAHs by Terrestrial Invertebrates, in *PAHs: An Ecotoxicological Perspective*, P. E. T. Douben, Ed. (Wiley, 2003), pp. 173–190.
33. J. P. Meador, J. E. Stein, W. L. Reichert, U. Varanasi, Bioaccumulation of polycyclic aromatic hydrocarbons by marine organisms. *Rev. Environ. Contam. Toxicol.* **143**, 79–165 (1995).
34. M. Octaviani, I. Stemmler, G. Lammel, H. F. Graf, Atmospheric transport of persistent organic pollutants to and from the Arctic under present-day and future climate. *Environ. Sci. Technol.* **49**, 3593–3602 (2015).
35. T. Berkemeier, M. Shiraiwa, U. Pöschl, T. Koop, Competition between water uptake and ice nucleation by glassy organic aerosol particles. *Atmos. Chem. Phys.* **14**, 12513–12531 (2014).
36. M. Song, P. F. Liu, S. J. Hanna, Y. J. Li, S. T. Martin, A. K. Bertram, Relative humidity-dependent viscosities of isoprene-derived secondary organic material and atmospheric implications for isoprene-dominant forests. *Atmos. Chem. Phys.* **15**, 5145–5159 (2015).
37. M. Shiraiwa, A. Zuend, A. K. Bertram, J. H. Seinfeld, Gas-particle partitioning of atmospheric aerosols: Interplay of physical state, non-ideal mixing and morphology. *Phys. Chem. Chem. Phys.* **15**, 11441–11453 (2013).
38. P. Shahpoury, G. Lammel, A. Albinet, A. Sofuoğlu, Y. Dumanoğlu, S. C. Sofuoğlu, Z. Wagner, V. Zdimal, Evaluation of a conceptual model for gas-particle partitioning of polycyclic aromatic hydrocarbons using polyparameter linear free energy relationships. *Environ. Sci. Technol.* **50**, 12312–12319 (2016).
39. Y. Cheng, H. Su, T. Koop, E. Mikhailov, U. Pöschl, Size dependence of phase transitions in aerosol nanoparticles. *Nat. Commun.* **6**, 5923 (2015).
40. Y. Cheng, G. Zheng, C. Wei, Q. Mu, B. Zheng, Z. Wang, M. Gao, Q. Zhang, K. He, G. Carmichael, U. Pöschl, H. Su, Reactive nitrogen chemistry in aerosol water as a source of sulfate during haze events in China. *Sci. Adv.* **2**, e1601530 (2016).
41. G. A. Grell, S. E. Peckham, R. Schmitz, S. A. McKeen, G. Frost, W. C. Skamarock, B. Eder, Fully coupled “online” chemistry within the WRF model. *Atmos. Environ.* **39**, 6957–6975 (2005).
42. *WRF-Chem Version 3.6.1 User's Guide* (National Center for Atmospheric Research, 2014).
43. E. Roeckner, G. Bäuml, L. Bonaventura, R. Brokopf, M. Esch, M. Giorgetta, S. Hagemann, I. Kirchner, L. Kornblueh, E. Manzini, A. Rhodin, U. Schlese, U. Schulzweida, A. Tompkins, “The atmospheric general circulation model ECHAM 5. Part I: Model description” (MPI-Report No. 349, Max Planck Institute for Meteorology, 2003).
44. P. Jöckel, A. Kerkweg, A. Pozzer, R. Sander, H. Tost, H. Riede, A. Baumgaertner, S. Gromov, B. Kern, Development cycle 2 of the Modular Earth Submodel System (MESSy2). *Geosci. Model Dev.* **3**, 717–752 (2010).
45. H. Shen, Y. Huang, R. Wang, D. Zhu, W. Li, G. Shen, B. Wang, Y. Zhang, Y. Chen, Y. Lu, H. Chen, T. Li, K. Sun, B. Li, W. Liu, J. Liu, S. Tao, Global atmospheric emissions of polycyclic aromatic hydrocarbons from 1960 to 2008 and future predictions. *Environ. Sci. Technol.* **47**, 6415–6424 (2013).
46. G. Janssens-Maenhout, M. Crippa, D. Guizzardi, F. Dentener, M. Muntean, G. Pouliot, T. Keating, Q. Zhang, J. Kurokawa, R. Wankmüller, H. Denier van der Gon, J. J. P. Kuenen, Z. Klimont, G. Frost, S. Darras, B. Koffi, M. Li, HTAP_v2.2: A mosaic of regional and global emission grid maps for 2008 and 2010 to study hemispheric transport of air pollution. *Atmos. Chem. Phys.* **15**, 11411–11432 (2015).
47. R. Lohmann, G. Lammel, Adsorptive and absorptive contributions to the gas-particle partitioning of polycyclic aromatic hydrocarbons: State of knowledge and recommended parametrization for modeling. *Environ. Sci. Technol.* **38**, 3793–3803 (2004).
48. E. Galarneau, P. A. Makar, Q. Zheng, J. Narayan, J. Zhang, M. D. Moran, M. A. Bari, S. Pathela, A. Chen, R. Chlumsky, PAH concentrations simulated with the AURAMS-PAH chemical transport model over Canada and the USA. *Atmos. Chem. Phys.* **14**, 4065–4077 (2014).
49. W. Klöpffer, B. O. Wagner, K. G. Steinhäuser, *Atmospheric Degradation of Organic Substances: Persistence, Transport Potential, Spatial Range* (Wiley, 2008).
50. W. A. Jury, W. F. Spencer, W. J. Farmer, Behavior assessment model for trace organics in soil: I. Model description. *J. Environ. Qual.* **12**, 558–564 (1983).
51. G. Lammel, A. M. Sehill, T. C. Bond, J. Feichter, H. Grassl, Gas/particle partitioning and global distribution of polycyclic aromatic hydrocarbons—A modelling approach. *Chemosphere* **76**, 98–106 (2009).
52. M. Shiraiwa, C. Pfrang, T. Koop, U. Pöschl, Kinetic multi-layer model of gas-particle interactions in aerosols and clouds (KM-GAP): Linking condensation, evaporation and chemical reactions of organics, oxidants and water. *Atmos. Chem. Phys.* **12**, 2777–2794 (2012).
53. J. Y. Kim, J. Y. Lee, S.-D. Choi, Y. P. Kim, Y. S. Ghim, Gaseous and particulate polycyclic aromatic hydrocarbons at the Gosan background site in East Asia. *Atmos. Environ.* **49**, 311–319 (2012).
54. K. Tørseth, W. Aas, K. Breivik, A. M. Fjæraa, M. Fiebig, A. G. Hjellbrekke, C. Lund Myhre, S. Solberg, K. E. Yttri, Introduction to the European Monitoring and Evaluation Programme (EMEP) and observed atmospheric composition change during 1972–2009. *Atmos. Chem. Phys.* **12**, 5447–5481 (2012).

55. E. Galarneau, T. F. Bidleman, P. Blanchard, Seasonality and interspecies differences in particle/gas partitioning of PAHs observed by the Integrated Atmospheric Deposition Network (IADN). *Atmos. Environ.* **40**, 182–197 (2006).
56. H. Hung, R. Kallenborn, K. Breivik, Y. Su, E. Brorström-Lundén, K. Olafsdottir, J. M. Thorlacius, S. Leppänen, R. Bossi, H. Skov, S. Manø, G. W. Patton, G. Stern, E. Sverko, P. Fellin, Atmospheric monitoring of organic pollutants in the Arctic under the Arctic Monitoring and Assessment Programme (AMAP): 1993–2006. *Sci. Total Environ.* **408**, 2854–2873 (2010).
57. A. Ding, X. Huang, C. Fu, *Air pollution and weather interaction in East Asia* (Oxford Research Encyclopedia of Environmental Science, 2017).
58. A. Ding, T. Wang, L. Xue, J. Gao, A. Stohl, H. Lei, D. Jin, Y. Ren, X. Wang, X. Wei, Y. Qi, J. Liu, X. Zhang, Transport of north China air pollution by midlatitude cyclones: Case study of aircraft measurements in summer 2007. *J. Geophys. Res.* **114**, D08304 (2009).
59. A. Stohl, Z. Klimont, S. Eckhardt, K. Kupiainen, V. P. Shevchenko, V. M. Kopeikin, A. N. Novigatsky, Black carbon in the Arctic: The underestimated role of gas flaring and residential combustion emissions. *Atmos. Chem. Phys.* **13**, 8833–8855 (2013).
60. P. Winiger, A. Andersson, S. Eckhardt, A. Stohl, Ö. Gustafsson, The sources of atmospheric black carbon at a European gateway to the Arctic. *Nat. Commun.* **7**, 12776 (2016).

Acknowledgments: We thank Q. Zhang, Y. Zhang, and G. Zheng (Tsinghua University, China) for sampling, and P. Přibyllová and O. Audy (Masaryk University, Czech Republic) for chemical analysis at the Xianghe site. We also acknowledge Y.-S. Ghim (Hankuk University of Foreign Studies, Korea) for sharing of BaP concentration data at the Gosan site. **Funding:** We acknowledge the National Natural Science Foundation of China (91644218 and 41330635),

NSF (AGS-1654104), U.S. Department of Energy (DE-SC0018349), and Czech Science Foundation (P503 16-11537S). This work was supported by the Max Planck Society (MPG). Y.C. would also like to thank the Minerva Program of MPG. **Author contributions:** Y.C., H.S., U.P., and G.L. conceived the study. M.S., Y.C., H.S., and U.P. developed the temperature-dependent ROI-T scheme for model implementation. Q.M. incorporated new PAH module into the regional model WRF-Chem and performed the model simulation and data analyses. M.O. incorporated new PAH module into the global model EMAC and performed the model simulation and data analyses. Y.C., H.S., and Q.M. analyzed and interpreted results. N.M. contributed to data analysis and visualization. A.D. contributed to the transport process analysis and relevant discussion in the Supplementary Materials. All coauthors discussed the results. H.S., Y.C., and Q.M. wrote the manuscript with input from all coauthors. **Competing interests:** The authors declare that they have no competing interests. **Data and materials availability:** All data needed to evaluate the conclusions in the paper are present in the paper and/or the Supplementary Materials. Additional data related to this paper may be requested from the authors.

Submitted 21 August 2017

Accepted 9 February 2018

Published 21 March 2018

10.1126/sciadv.aap7314

Citation: Q. Mu, M. Shiraiwa, M. Octaviani, N. Ma, A. Ding, H. Su, G. Lammel, U. Pöschl, Y. Cheng, Temperature effect on phase state and reactivity controls atmospheric multiphase chemistry and transport of PAHs. *Sci. Adv.* **4**, eaap7314 (2018).

Temperature effect on phase state and reactivity controls atmospheric multiphase chemistry and transport of PAHs

Qing Mu, Manabu Shiraiwa, Mega Octaviani, Nan Ma, Aijun Ding, Hang Su, Gerhard Lammel, Ulrich Pöschl and Yafang Cheng

Sci Adv 4 (3), eaap7314.
DOI: 10.1126/sciadv.aap7314

ARTICLE TOOLS

<http://advances.sciencemag.org/content/4/3/eaap7314>

SUPPLEMENTARY MATERIALS

<http://advances.sciencemag.org/content/suppl/2018/03/19/4.3.eaap7314.DC1>

REFERENCES

This article cites 55 articles, 4 of which you can access for free
<http://advances.sciencemag.org/content/4/3/eaap7314#BIBL>

PERMISSIONS

<http://www.sciencemag.org/help/reprints-and-permissions>

Use of this article is subject to the [Terms of Service](#)

Science Advances (ISSN 2375-2548) is published by the American Association for the Advancement of Science, 1200 New York Avenue NW, Washington, DC 20005. The title *Science Advances* is a registered trademark of AAAS.

Copyright © 2018 The Authors, some rights reserved; exclusive licensee American Association for the Advancement of Science. No claim to original U.S. Government Works. Distributed under a Creative Commons Attribution NonCommercial License 4.0 (CC BY-NC).